# Encapsulation of 2D MoS$_2$ Nanosheets into 1D Carbon Nanobelts as Anodes with Enhanced Lithium/Sodium Storage Properties

Bingqing Ye[1], Lei Xu[1], Wenbo Wu[1], Yuliang Ye[1], Zunxian Yang[*1,2], Jingwei Ai[1], Yinglin Qiu[1], Zhipeng Gong[1], Yuanqing Zhou[1], Qiaocan Huang[1], Zihong Shen[1], Fushan Li[1,2], Tailiang Guo[1,2], Sheng Xu[1,2]

[1]National & Local United Engineering Laboratory of Flat Panel Display Technology, Fuzhou University, Fuzhou 350108, P. R. China.

[2]Mindu Innovation Laboratory, Fujian Science & Technology Innovation Laboratory For Optoelectronic Information of China, Fuzhou,350108, P.R. China

**Supporting Information**

**Captions**

**Table S1** A comparison of the cycling performance of MoS$_2$@C with the recently reported MoS$_2$/C- based anode materials for Li-ion batteries in other literature.

**Fig.S1** XRD patterns of pure α-MoO$_3$ NBs, MoO$_3$@C-22 NBs, MoO$_3$@C-23 NBs,

* Corresponding author should be addressed. Tel.: +86 591 8789 3299; Fax: +86 591 8789 2643
E-mail: yangzunxian@hotmail.com          (Z. Yang)

MoO$_3$@C-24 NBs, and MoO$_3$@C-25 NBs, respectively.

**Fig.S2** TGA curve of MoS$_2$@C-23 NBs.

**Fig.S3 (a)** N2 adsorption-desorption isotherms and **(b)** pore size distribution of MoS$_2$@C-23 NBs.

**Fig.S4 (a)** Low-magnification and **(b)** High-magnification SEM image of pure MoS$_2$ nanosheets.

**Fig.S5 (a, b)** Low-magnification and **(c, d)** High-magnification TEM images of MoS$_2$@C-23 NBs.

**Fig.S6** SEM images of **(a)** MoO$_3$@C-22 NBs, **(b)** MoO$_3$@C-24 NBs, **(c)** MoO$_3$@C-25 NBs, **(d)** MoS$_2$@C-22 NBs, **(e)** MoS$_2$@C-24 NBs, and **(f)** MoS$_2$@C-25 NBs.

**Fig.S7 (a)** TEM image of MoO$_3$@C-13 NBs. **(b)** TEM image of MoO$_3$@C-33 NBs.

**Fig.S8 (a, b)** SEM images of MoS$_2$@C-13 NBs. **(c)** Low-magnification and **(d)** High-magnification SEM images of MoS$_2$@C-33 NBs.

**Fig.S9** XRD patterns of MoS$_2$@C-13 NBs and MoS$_2$@C-33 NBs.

**Fig.S10 (a, b)** SEM images, **(c)** TEM image, **(d)** HRTEM image, **(e)** XRD patterns, and **(f-i)** EDS mapping of C@MoS$_2$.

**Fig.S11** Rate capability of MoS$_2$@C-22 NBs, MoS$_2$@C-24 NBs, and MoS$_2$@C-25 NBs cycled at various rates from 0.1 to 2.0 Ag$^{-1}$.

**Fig.S12** Rate capability of MoS$_2$@C cycled at various rates from 0.1 to 2.0 Ag$^{-1}$.

**Fig.S13** Cycling performance of MoS$_2$@C-22 NBs, MoS$_2$@C-24 NBs, and MoS$_2$@C-25 NBs at a current density of 0.2 Ag$^{-1}$.

**Fig. S14** Cycling performance of C@MoS$_2$ at a current density of 0.2 Ag$^{-1}$.

**Fig. S15** SEM images of MoS$_2$@C-23 NBs after 200 cycles.

**Fig. S16 (a)** EIS and **(b)** plots of Z' vs. $\omega^{-1/2}$ of MoS$_2$@C-22 NBs, MoS$_2$@C-24 NBs, and MoS$_2$@C-25 NBs.

**Fig. S17 (a)** EIS and **(b)** plots of Z' vs. $\omega^{-1/2}$ of C@MoS$_2$.

**Table S1.**

| MoS$_2$/C-based anode materials | Current density (mAg$^{-1}$) | (Cycles) | Capacity (mAhg$^{-1}$) | Reference |
|---|---|---|---|---|
| MoS$_2$@NSC nanoprisms | 100 | 300 | 800 | [1] |
| 3DANCNT@MoS$_2$ composite | 200<br>1600 | 200<br>200 | 893.4<br>645 | [2] |
| MoS$_2$/N-CNT | 200 | 100 | 1115 | [3] |
| MoS$_2$@C nanospheres | 100<br>2000 | 100<br>500 | 1119<br>530 | [4] |
| CNT@MoS$_2$@C | 100 | 200 | 982 | [5] |
| MoS$_2$ @PZS-C nanospheres | 100 | 100 | 1245 | [6] |
| MoS$_2$@C/MoS$_2$ core−Sheath nanowires | 100 | 150 | 838 | [7] |
| MoS$_2$ nanosheets/ N, O-codoped carbon matrix | 67 | 100 | 946.3 | [8] |
| Bowl-like C@MoS$_2$ nanocomposites | 100<br>1000 | 100<br>1000 | 798<br>526 | [9] |
| MoS$_2$/N-doped carbon nanobelts | 100<br>1000 | 100<br>500 | 901<br>675 | [10] |
| C@MoS$_2$@NC hollow spheres | 100 | 10 | 747 | [11] |
| 3D FNC-MoS$_2$ nanospheres | 100<br>1200 | 50<br>400 | 920<br>700 | [12] |
| NC@MoS$_2$@C nanotubes | 100<br>1000 | 100<br>500 | 663.3<br>703.5 | [13] |
| MoS$_2$-PVP@NC nanospheres | 1000 | 300 | 607.1 | [14] |
| MoS$_2$@C-23 NBs | 200<br>1000 | 200<br>800 | 1189<br>626 | This work |
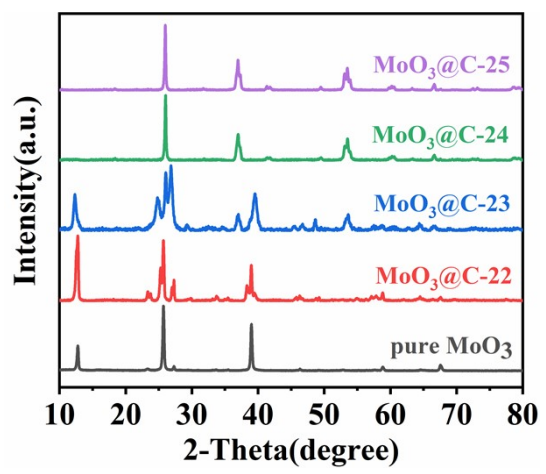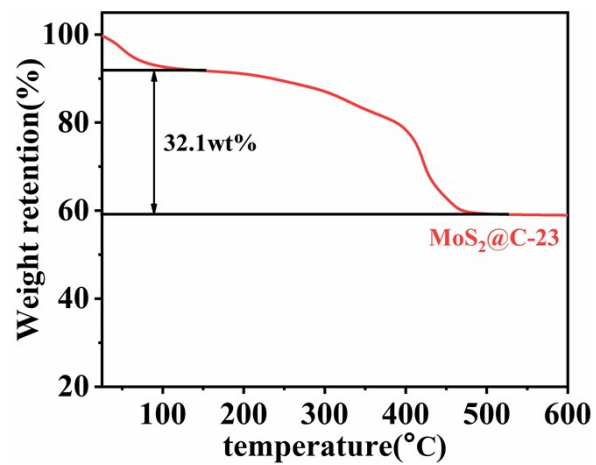
**Fig.S1**

**Fig.S2**
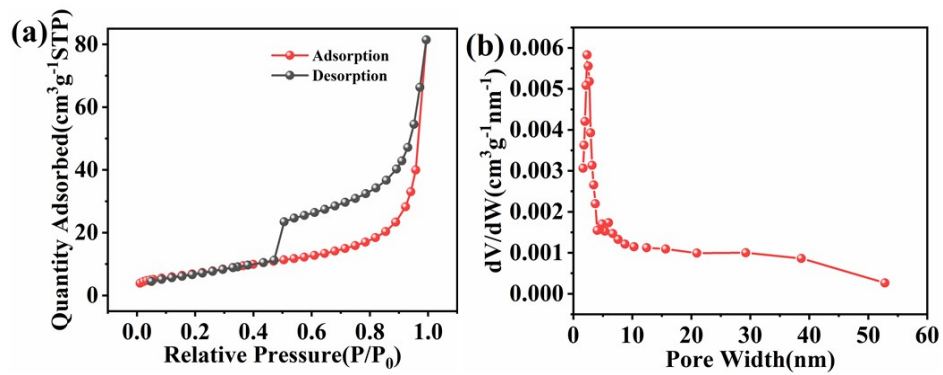
**Fig.S3**
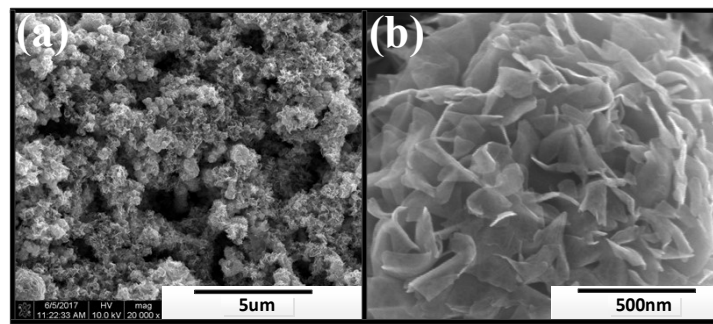
**Fig.S4**
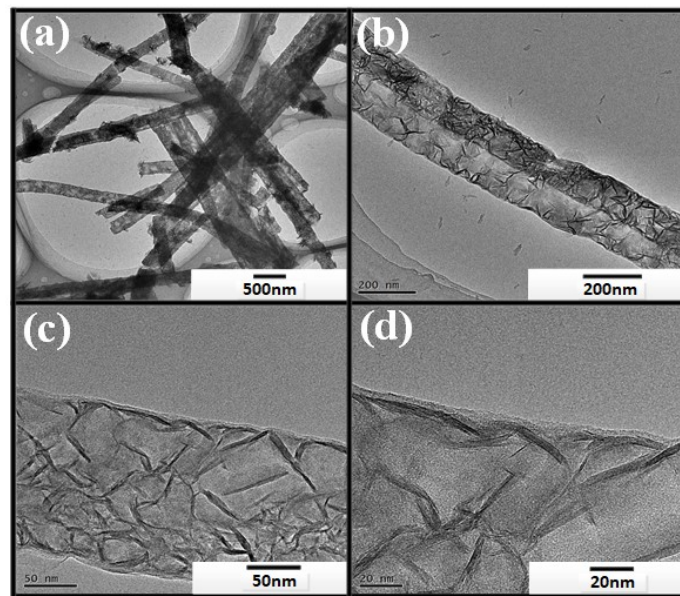
**Fig.S5**
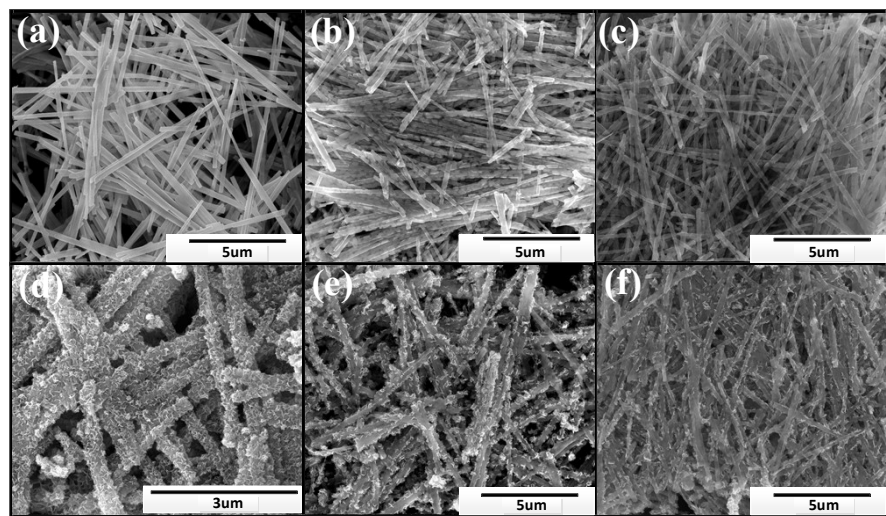
**Fig.S6**
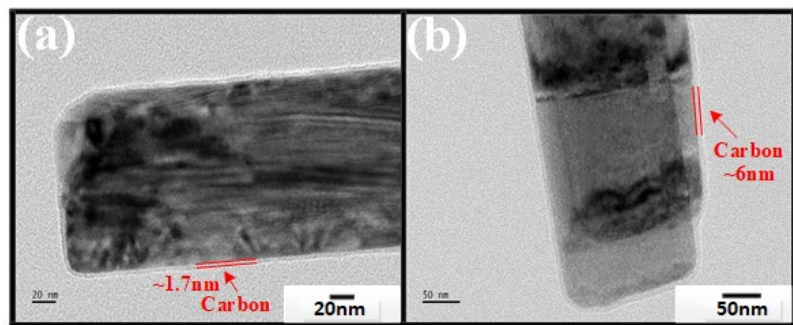
**Fig.S7**
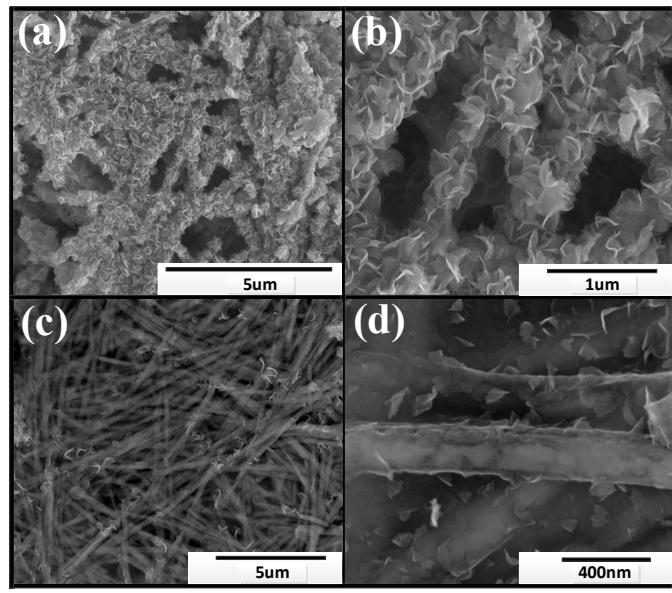
**Fig.S8**
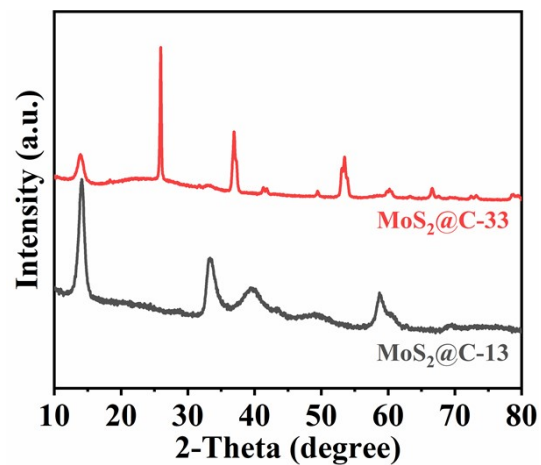
**Fig.S9**
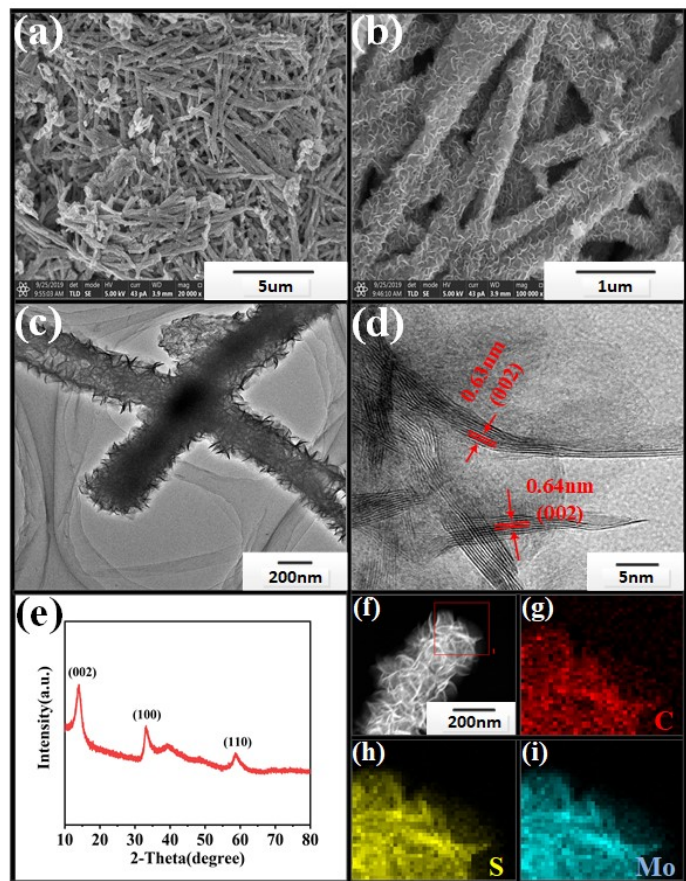
**Fig.S10**
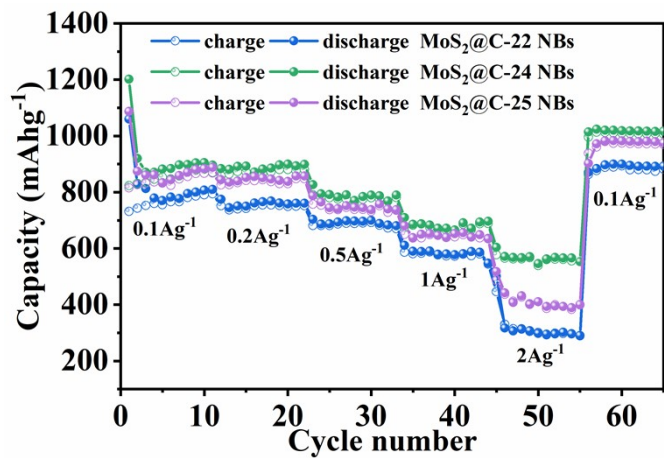
**Fig.S11**
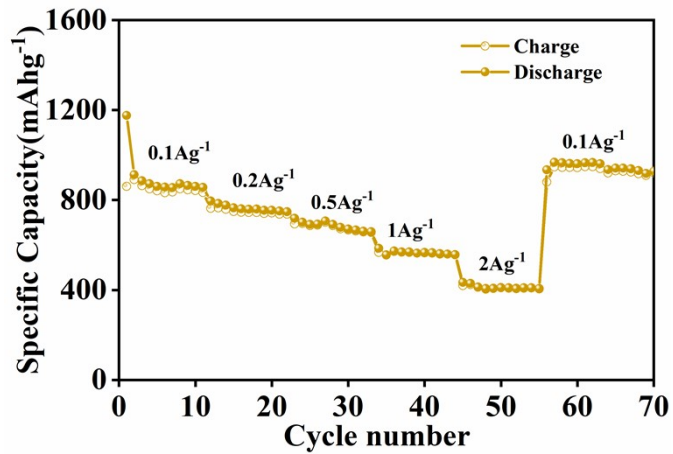
**Fig.S12**
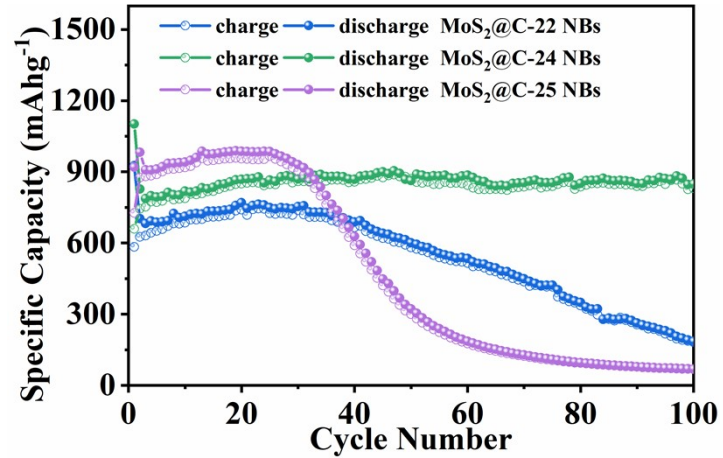
**Fig.S13**
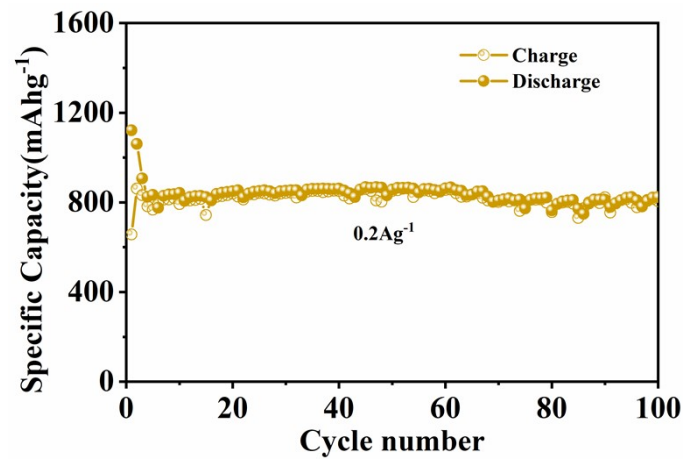
**Fig. S14**
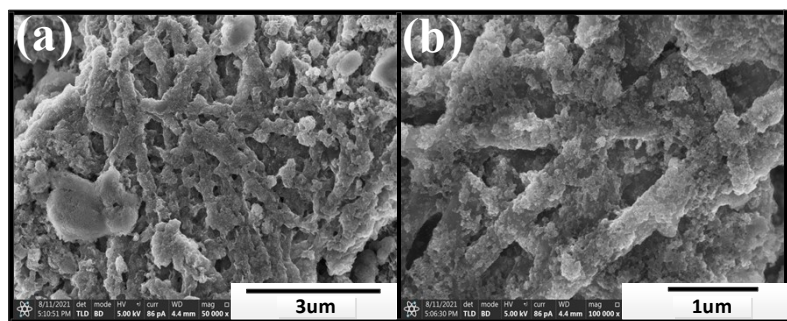
**Fig. S15**
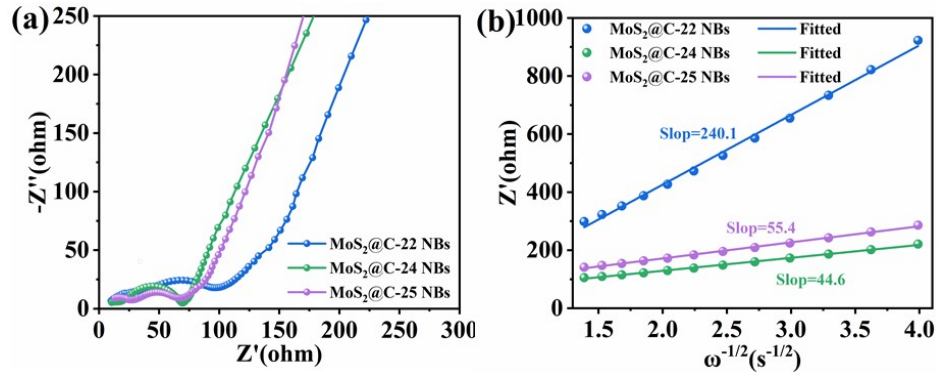
**Fig. S16**
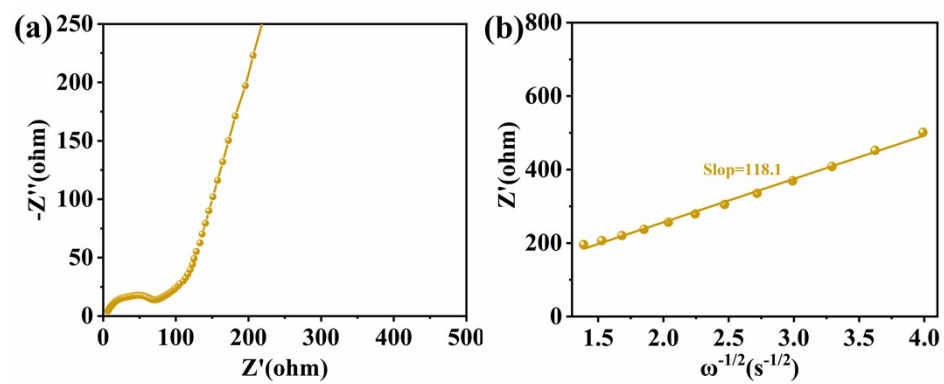
**Fig. S17**

**References**

**[1]** Y. Liu, J. Zhu, J. Xu, S. Liu, L. Li, C. Zhang, T. Liu, High-temperature solvent-free sulfidation of MoO3 confined in a polypyrrole shell: MoS2 nanosheets encapsulated in a nitrogen, sulfur dual-doped carbon nanoprism for efficient lithium storage. **Nanoscale**, **2018**, **10**(16): 7536-7543.

**[2]** X. J. Zhao, G. Wang, X. J. Liu, X. L. Zheng, H. Wang, Ultrathin MoS2 with expanded interlayers supported on hierarchical polypyrrole-derived amorphous N-doped carbon tubular structures for high-performance Li/Na-ion batteries. **Nano Research**, **2018**, **11**(7): 3603-3618.

**[3]** T. J. Wu, M. J. Jing, Y. Liu, X. B. Ji, Binding low crystalline MoS2 nanoflakes on nitrogen-doped carbon nanotube: towards high-rate lithium and sodium storage. **Journal of Materials Chemistry A**, **2019**, **7**(11): 6439-6449.

**[4]** J. G. Wang, H. Y. Liu, R. Zhou, X. R. Liu, B. Q. Wei, Onion-like nanospheres organized by carbon encapsulated few-layer MoS2 nanosheets with enhanced lithium storage performance. **Journal of Power Sources**, **2019**, **413**: 327-333.

**[5]** Z. J. Zhang, H. L. Zhao, Y. Q. Teng, X. W. Chang, Q. Xia, Z. L. Li, J. J. Fang, Z. H. Du, K. Swierczek, Carbon-Sheathed MoS2 Nanothorns Epitaxially Grown on CNTs: Electrochemical Application for Highly Stable and Ultrafast Lithium Storage. **Advanced Energy Materials**, **2018**, **8**(7): 1700174.

**[6]** Z. P. Zhou, F. Chen, L. Wu, T. R. Kuang, X. H. Liu, J. T. Yang, P. Fan, Z. D. Fei, Z. P. Zhao, M. Q. Zhong, Heteroatoms-doped 3D carbon nanosphere cages embedded

with MoS2 for lithium-ion battery. **Electrochimica Acta**, **2020**, **332**: 135490.

[7] H. H. Sun, J. G. Wang, X. Z. Zhang, C. J. Li, F. Liu, W. J. Zhu, W. Hua, Y. Y. Li, M. H. Shao, Nanoconfined Construction of MoS2@C/MoS2 Core-Sheath Nanowires for Superior Rate and Durable Li-Ion Energy Storage. **Acs Sustainable Chemistry & Engineering**, **2019**, **7**(5): 5346-5354.

[8] M. S. Han, Z. J. Lin, J. Yu, Ultrathin MoS2 nanosheets homogenously embedded in aN,O-codoped carbon matrix for high-performance lithium and sodium storage. **Journal of Materials Chemistry A**, **2019**, **7**(9): 4804-4812.

[9] X. E. Zhang, X. Chen, H. J. Ren, G. W. Diao, M. Chen, S. W. Chen, Bowl-like C@MoS2 Nanocomposites as Anode Materials for Lithium-Ion Batteries: Enhanced Stress Buffering and Charge/Mass Transfer. **Acs Sustainable Chemistry & Engineering**, **2020**, **8**(27): 10065-10072.

[10] H. H. Sun, J. G. Wang, W. Hua, J. J. Wang, D. Nan, B. H. Guo, Hierarchical MoS2/N-doped carbon nanobelts assembled by interlaced nanosheets as high performance Li-ion battery anode. **Journal of Alloys and Compounds**, **2020**, **821**: 153339.

[11] F. Z. Wang, F. G. Li, L. Ma, M. J. Zheng, Few-Layer MoS2 Nanosheets Encapsulated in N-Doped Carbon Hollow Spheres as Long-Life Anode Materials for Lithium-Ion Batteries. **Chemistry-a European Journal**, **2019**, **25**(64): 14598-14603.

[12] Xin Wang, Siming Fei, Shoushuang Huang, Chenghao Wu, Junru Zhao, Zhiwen Chen, Kajsa Uvdal, Zhangjun Hu, MoS2 nanosheets inlaid in 3D fibrous N-doped carbon spheres for lithium-ion batteries and electrocatalytic hydrogen evolution

reaction. **Carbon**, **2019**, **150**: 363-370.

**[13]** J. G. Zong, F. Wang, J. P. Zhao, X. Fan, M. S. Zhao, S. Yang, X. P. Song, Rational design of strong chemical coupling carbon coated N-doped C@MoS2@C nanotubes for high-performance lithium storage. **Journal of Alloys and Compounds**, **2021**, **861**: 157981.

**[14]** J. Bai, B. C. Zhao, X. Wang, H. Y. Ma, K. Z. Li, Z. T. Fang, H. Li, J. M. Dai, X. B. Zhu, Y. P. Sun, Yarn ball-like MoS2 nanospheres coated by nitrogen-doped carbon for enhanced lithium and sodium storage performance. **Journal of Power Sources**, **2020**, **465**: 228282.